Eur. J. Med. Chem. 34 (1999) 809–824

Original article

5-Substituted UTP derivatives as $P2Y_2$ receptor agonists[#]

Bernd H.A. Knoblauch[a,d], Christa E. Müller[a,c]*, Leif Järlebark[d], Grace Lawoko[d], Thomas Kottke[b], Martin A. Wikström[e], Edith Heilbronn[d]

[a]*Institut für Pharmazie und Lebensmittelchemie, Pharmazeutische Chemie, Universität Würzburg, Am Hubland, D-97074 Würzburg, Germany*
[b]*Institut für Anorganische Chemie, Universität Würzburg, Am Hubland, D-97074 Würzburg, Germany*
[c]*Universität Bonn, Pharmazeutisches Institut, Pharmazeutische Chemie Poppelsdorf, Germany*
[d]*Stockholm University, Department of Neurochemistry and Neurotoxicology, Arrhenius Laboratories of Natural Sciences, Stockholm, Sweden*
[e]*Karolinska Institute, Nobel Institute for Neurophysiology, Department of Neuroscience, Stockholm, Sweden*

(Received 8 February 1999; revised 30 April 1999; accepted 6 May 1999)

Abstract – A series of 5-alkyl-substituted UTP derivatives, which had been synthesized previously with a moderate degree of purity, was resynthesized, purified, and characterized. Synthetic and purification procedures were optimized. New spectroscopic data, including ^{13}C- and ^{31}P NMR data, are presented. Phosphorylation reactions yielded a number of side products, such as the 2′-, 3′-, and 5′-monophosphates, the 2′,3′-cyclic monophosphates, and the 2′,3′-cyclic phosphates of the 5′-triphosphates. Furthermore, raw products were contaminated with inorganic phosphates, including cyclometatriphosphate, phosphate, and pyrophosphate. The uracil nucleotides were investigated for their potency to increase intracellular calcium concentrations by stimulation of $P2Y_2$ receptors ($P2Y_2R$) on NG108–15 cells, a mouse neuroblastoma × glioma cell line, and in human basal epithelial airway cells, including a cystic fibrosis (CF/T43) cell line. UTP exhibited EC_{50} values of ca. 1 μM (in NG108–15 cells) and of 0.1 μM (in CF/T43 cells), respectively. 5-Substituted UTP derivatives were agonists at the $P2Y_2R$, but were less potent than UTP. 5-Ethyl-UTP, for example, exhibited an EC_{50} value of 99 μM at $P2Y_2R$ of NG108–15 cells and proved to be a full agonist. With increasing volume of the 5-substituent of UTP derivatives, $P2Y_2$ activity decreased. © 1999 Éditions scientifiques et médicales Elsevier SAS

$P2Y_2$ receptor agonists / P_{2U} receptor agonists / UTP analogues / pyrimidine nucleotides / cystic fibrosis

1. Introduction

Membrane receptors for endogenous nucleotides, such as ATP and UTP *(figure 1)* belong to the purine/pyrimidine receptor family. Purine receptors are subdivided into two separate families, the adenosine receptors, or P1-receptors (P1R), and the purine and pyrimidine nucleotide receptors or P2-receptors (P2R) [1, 2]. The growing family of known P2 receptors comprises subfamilies of ionotropic (P2X) and metabotropic (P2Y) receptors. While P2XR subtypes appear to be activated exclusively by adenine nucleotides, subtypes of P2YR exist, including $P2Y_2$, $P2Y_4$, $P2Y_6$, at which uracil nucleotides, namely UTP or UDP, show activity and may act as physiological agonists. The $P2Y_2R$ is a ubiquitously expressed UTP-sensitive P2YR subtype, also known as $P_{2U}R$ [3]. ATP and UTP are equipotent as agonists at the $P2Y_2R$. It has recently been found that the impaired chloride transport in the bronchi of patients suffering from cystic fibrosis can be bypassed by stimulation of a $P2Y_2R$ to activate an alternative chloride channel [4]. UTP is currently under development as a

[#] Preliminary results were presented at the Joint Meeting of the German and Swiss Pharmaceutical Societies in Zürich, Switzerland, 1997, and at the International Symposium on Adenosine and Adenine Nucleotides in Ferrara, Italy (abstract in *Drug Dev. Res.* 43 (1998) 34).

* Correspondence and reprints
Dr Christa Müller, Pharmazeutisches Institut der Universität Bonn, Pharmazeutische Chemie Poppelsdorf, Kreuzbergweg 26, D-53115 Bonn.

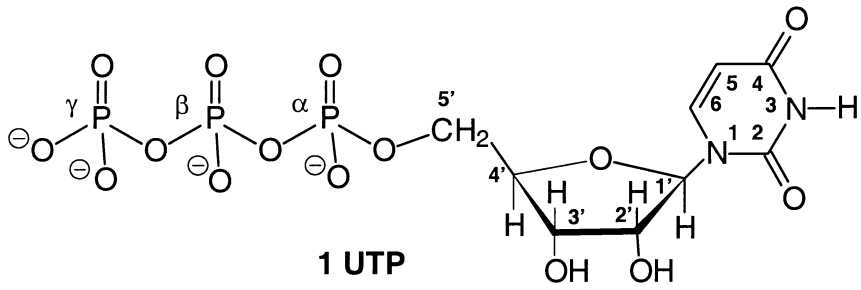

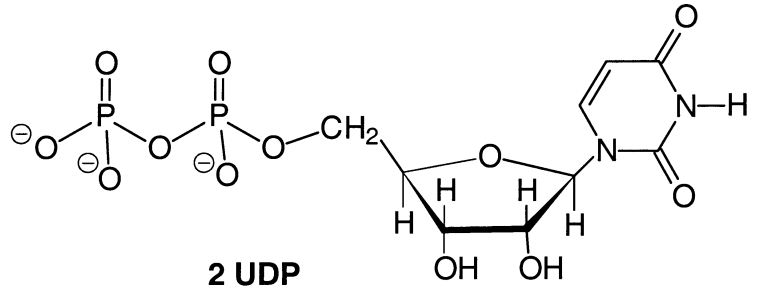

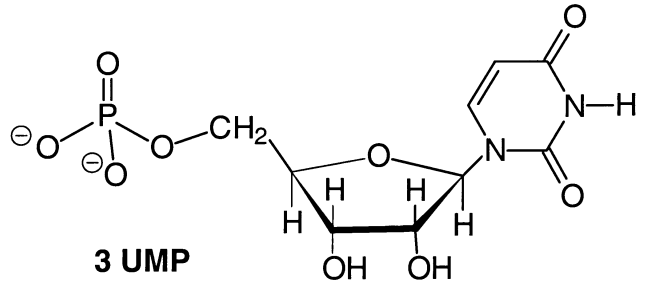

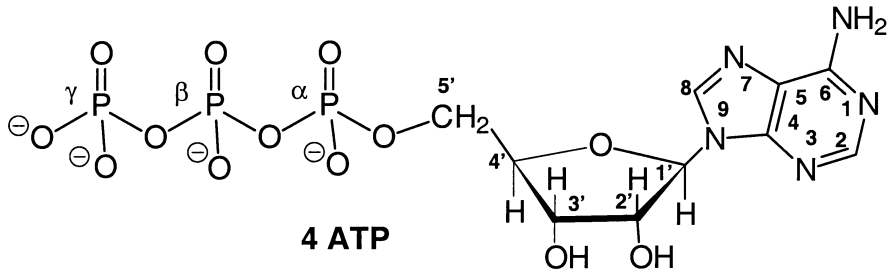

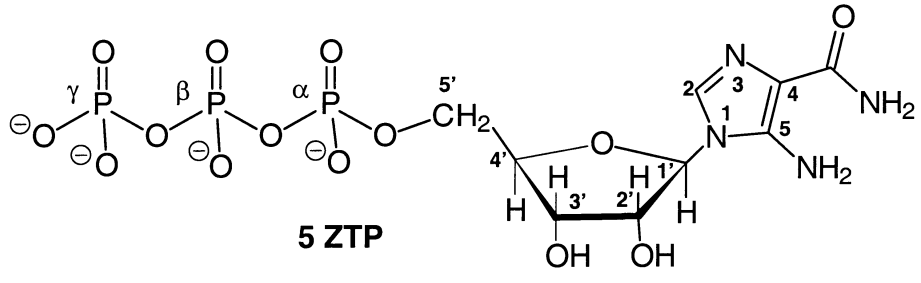

Figure 1. Structures of standard nucleotides.

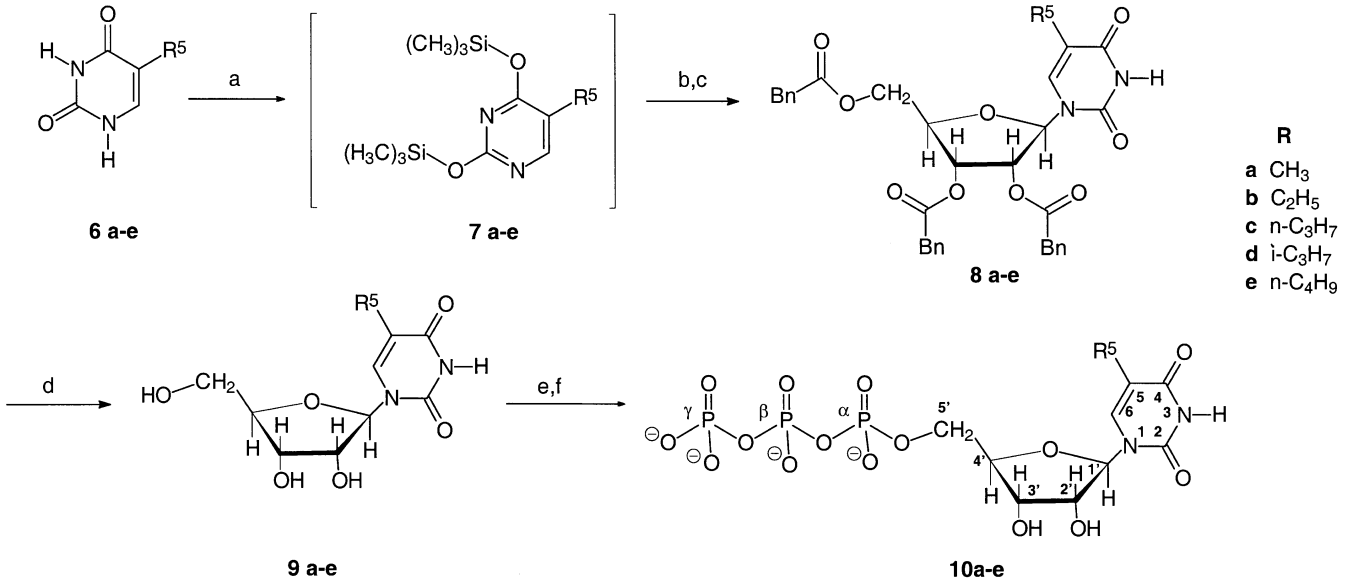

(a) HMDS, trimethylsilylchloride (or $(NH_4)_2SO_4$); (b) 1-O-acetyl-2,3,5-tri-O-benzoyl-β-D-ribose, $SnCl_4$; (c) $NaHCO_3$, H_2O; (d) $NaOCH_3$, MeOH; (e) $POCl_3$, trimethyl phosphate; (f) tributylamine, tributylammonium pyrophosphate, DMF

Figure 2. Preparation of 5-substituted UTP derivatives.

novel therapeutic agent for the symptomatic treatment of cystic fibrosis.

Only few $P2Y_2R$ agonists are known so far and structure-activity relationships for $P2Y_2R$ agonists are virtually unknown [5, 6]. In the present study we synthesized a series of 5-substituted UTP derivatives. We selected UTP as a lead structure to develop $P2Y_2R$ ligands, rather than ATP, because of the higher selectivity of UTP versus other P2R subtypes, e.g., P2XR. In addition, degradation products of ATP and analogues (adenosine and analogues) may interact with P1R (adenosine receptors), but not those of UTP and analogues [7]. The synthesized nucleotides were investigated in vitro for their potency to increase intracellular calcium concentration ($[Ca^{2+}]_i$) caused by a $P2Y_2R$-mediated stimulation of phospholipase C [8].

2. Chemistry

5-Alkyl-substituted UTP derivatives **10a–e** were synthesized according to published procedures with modifications *(figure 2)* [9–12]. Uracil derivatives **6a–e** were silylated using hexamethyldisilazane (HMDS) in the presence of trimethylsilylchloride, or ammonium sulfate, respectively. Derivatives with longer side chains dissolved faster in HMDS due to their higher lipophilicity as compared to those with smaller substituents. After complete dissolution, which indicated completion of the reaction, silylated uracil derivatives **7a–e** were characterized by their ^1H and ^{13}C NMR spectra *(table I)*. Condensation with 1-O-acetyl-2,3,5-tri-O-benzoyl-β-D-ribofuranose in the presence of tin(IV) chloride yielded nucleosides **8a–e**, essentially as described [9]. For 5-ethyl derivative **7b**, as an example, different reaction conditions were investigated. As solvents, 1,2-dichloroethane or acetonitrile were used. As Lewis acid catalysts tin(IV) chloride, or trimethylsilyltriflate, were applied. All different combinations gave very good yields of **8b** (80–90%). In 1,2-dichloroethane as a solvent, traces of N3-nucleoside were formed, which could be removed by silica gel column chromatography. Trimethylsilyltriflate was found not to be superior to tin(IV) chloride.

Hydrolysis was performed using a saturated aqueous sodium hydrogencarbonate solution. In our hands, potassium hydrogencarbonate showed no advantage over the sodium salt, in contrast to results reported by Szemo et al. [9]. Filtration over silica gel efficiently removed tin(IV) oxide hydrate formed during the reaction. The

Table I. ^{13}C-NMR data of silylated uracil derivatives (in $CDCl_3$) δ (ppm).

Compound	O-Si$(CH_3)_3$	C2	C4	C5	C6	R^5
7a	0.32	168.15	161.78	112.57	158.87	12.20
7b	0.29	167.84	161.69	118.33	157.90	13.42, 20.30
7c	0.26	167.87	161.66	116.75	158.63	13.67, 22.27, 28.91
7d	0.29	167.39	167.39	122.30	158.63	21.63, 26.24
7e	–0.41	167.26	161.08	116.08	157.83	13.08, 21.54, 25.91, 30.76

benzoylated nucleosides **8a–e** were deprotected via transesterification using methanolic sodium methylate solution. The formed benzoic acid methyl ester was conveniently removed by extraction with diethyl ether and subsequent lyophilization to yield the nucleosides **9a–e**. A recently described direct method for nucleoside synthesis [13], which does not require protection of the sugar, was investigated for the preparation of the 5-propyl derivative **10c**, but was not successful in our hands. At low temperatures no reaction occurred and the starting material was recovered. At temperatures over 80 °C only degradation was observed.

Nucleotides **10a–e** were prepared from nucleosides **9a–e** according to published procedures with slight modifications [9–12]. The lyophilized nucleosides were dissolved in dry trimethylphosphate and reacted with phosphorus oxychloride, with or without the addition of 1,8-bis(dimethylamino)naphthalene ('proton sponge'). The reactive intermediate phosphorodichloridate was coupled with a mixture of one equivalent of tri-n-butylamine and a five-fold excess of tri-n-butylammonium diphosphate in dimethylformamide to yield **10a–e** *(figure 2)*.

Nucleosides **8a–e** and **9a–e** were characterized by their ^{1}H NMR spectra, which were in accordance with published data [9]. In addition, ^{13}C NMR spectra were recorded *(tables II* and *III)*.

Crystals suitable for X-ray crystallography could be obtained from nucleosides **8b** and **8d**. The structure of nucleoside **8d** is shown in *figure 3* (see also *table VI*). Compound **8d** showed a nucleosidic torsion angle (O3-C5-N1-C1) of –133.22°. Thus, the nucleoside crystallized in the anti-conformation despite bulky 5- and 5′-substituents. The torsion angle γ about the exocyclic C8–C9 bond *(figure 3)* may be described as +sc (gauche/gauche). A vibrational disorder of the isopropyl side chain could be seen, probably facilitated by the low data collection temperature of 173 K. As an interesting feature, the sugar puckering in **8d** deviated from the conformation observed in unprotected 5-methyluridine [14], which adopted a C3′-endo conformation, while **8d** showed a sugar puckering that can be described as C1′-exo.

The synthesized nucleotides were purified by anion exchange chromatography using diethylaminoethyl-(DEAE-) Sephadex A25. The triethylammonium salts were converted to the corresponding sodium salts by dissolution in absolute methanol and subsequent precipitation by the addition of sodium iodide in acetone. The sodium salts were obtained as amorphous powders and therefore better to handle for biological tests than the triethylammonium salts, which were obtained as oily, transparent liquids.

Nucleotides were characterized by ^{13}C and ^{31}P NMR spectroscopy and plasma desorption mass spectrometry. Purity was determined by HPLC/UV and ^{31}P NMR spectroscopy *(tables III* and *IV)*. The combination of both methods proved to be important for purity control *(table IV)*.

Table II. ^{13}C-NMR data of protected nucleosides (in DMSO-d_6), δ (ppm).

Compound	C5′	C3′	C2′	C4′	C1′	$C_{aromat.}$	benzoyl	C5	C6	C2	C4	R^5
8a	63.7	70.7	73.1	78.8	88.5	128.4, 128.5, 128.7, 129.2, 129.3, 133.5, 133.7	164.4, 164.6, 165.5	110.1	136.9	150.9	162.9	11.9
8b	63.6	70.6	73.0	78.8	88.8	128.4, 128.6, 128.7, 129.2, 129.3, 133.5, 133.8	164.5, 164.6, 165.5	115.7	136.7	150.2	163.2	12.9, 19.5
8c	63.6	70.7	72.9	78.8	88.4	128.4, 128.5, 128.6, 129.3, 133.5, 133.6, 133.7	164.5, 164.6, 165.5	114.1	137.0	150.2	163.2	13.3, 21.1, 28.1
8d	63.7	70.6	73.0	78.8	89.4	128.4, 128.6, 128.7, 129.2, 129.3, 133.5, 133.8	164.5, 164.6, 165.5	119.9	136.1	150.0	162.9	21.0, 21.1, 25.5
8e	63.8	70.7	73.0	78.9	88.6	128.4, 128.5, 128.7, 129.2, 129.3, 133.5, 133.7	164.6, 164.7, 165.5	114.4	137.1	150.3	163.3	13.6, 21.7, 25.9, 30.2

Table III. ^{13}C-NMR data of nucleosides and nucleotides (in DMSO-d_6), δ (ppm).

Compound	C5′	C3′	C2′	C4′	C1′	C5	C6	C2	C4	R^5	$^3J_{C4'-P}$	$^2J_{C5'-P}$
9a	60.9	69.8	73.4	84.8	87.6	109.2	136.4	150.8	163.8	12.2		
9b	60.8	69.9	73.5	84.8	87.7	115.1	135.8	150.7	163.4	12.9, 19.7		
9c	60.8	69.8	73.4	84.7	87.8	113.2	136.4	150.6	163.3	12.9, 21.0, 28.4		
9d	60.7	69.9	73.8	84.7	88.1	119.4	134.9	150.4	163.0	21.2, 21.4, 25.4		
9e	60.8	69.8	73.6	84.8	87.8	113.5	136.4	150.7	163.5	12.9, 21.7, 25.9, 30.1		
10a	66.6	74.9	71.5	85.0	89.2	113.2	138.7	153.4	167.8	14.2	9.2	6.1
10b	66.7	74.6	71.6	85.1	89.0	118.9	138.2	153.2	167.1	12.1, 21.2	9.2	4.9
10c	66.8	64.8	71.6	85.1	89.2	117.2	139.0	153.3	167.3	14.4, 22.8, 29.6	9.2	6.1
10d	67.0	75.0	71.8	85.3	89.4	123.5	138.7	153.2	166.9	22.2, 22.5, 21.2	9.2	6.1
10e	66.9	74.8	71.6	85.1	89.3	117.7	138.9	153.8	167.5	14.9, 23.1, 27.5, 31.9	9.2	6.1

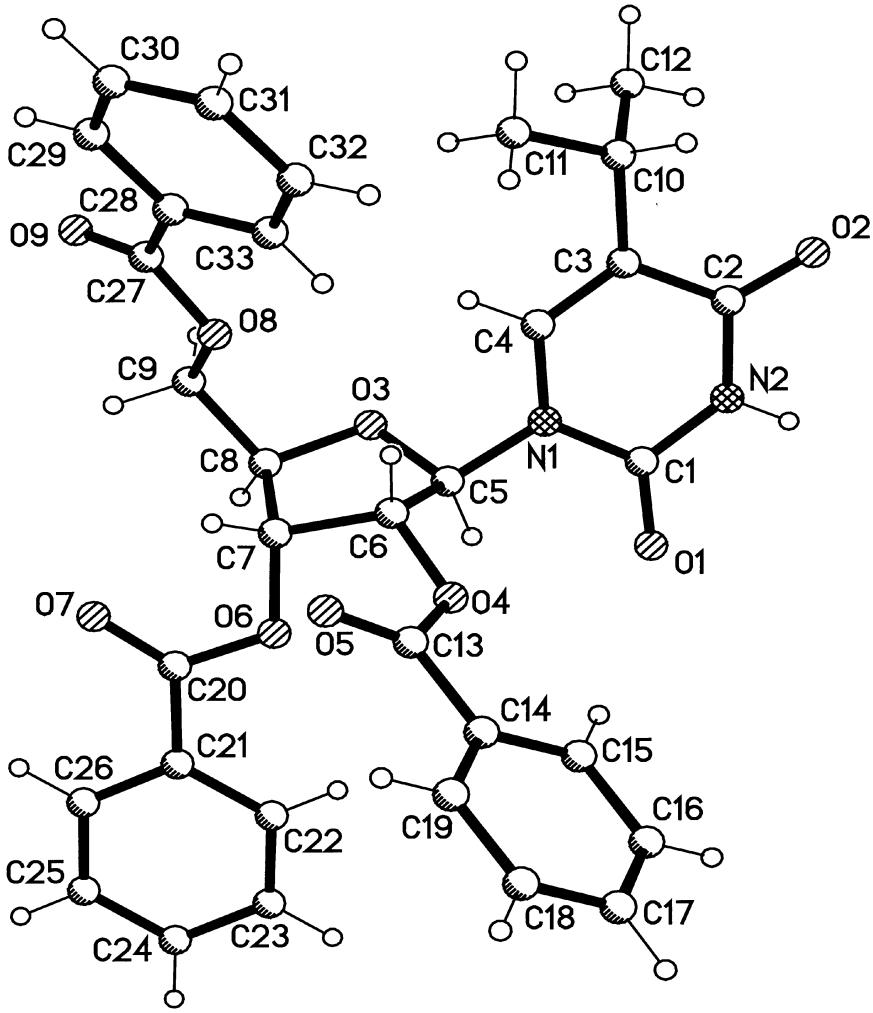

Figure 3. X-ray structure of nucleoside **8d.**

Table IV. ^{31}P-NMR (in D_2O), MS data and HPLC retention times of nucleotides **10a–e**, δ (ppm).

Compound	pH	^{31}P-NMR P_α	P_β	P_γ	MS[a] Mole Peak	Ion	HPLC (UV; λ =266 nm) System A[b] Retention time	(Purity)	System B[c] Retention time	(Purity)
10a	5.9	–10.69 d *J* = 19.6 Hz	–22.56 t *J* = 19.5 Hz	–10.04 d *J* = 19.5 Hz	496.9	$[M – H]^-$	13.51	(94 %)	7.56	(95 %)
10b	6.5	–10.26 d *J* = 19.6 Hz	–21.90 t *J* = 19.6 Hz	–9.26 d *J* = 19.5 Hz	511.1	$[M – H]^-$	21.88	(95 %)	7.82	(96 %)
10c	6.7	–10.38 d *J* = 19.6 Hz	–22.30 t *J* = 19.5 Hz	–9.05 d *J* = 19.5 Hz	524.9	$[M – H]^-$	25.97	(93 %)	8.01	(94 %)
10d	7.7	–10.58 d *J* = 20.0	–22.03 t *J* = 20.2 Hz	–7.14 d *J* = 19.8 Hz	524.8	$[M – H]^-$	17.36	(94 %)	9.40	(92 %)
10e	5.8	–10.98 d *J* = 20.2 Hz	–22.56 t *J* = 20.0 Hz	–10.04 d *J* = 19.8 Hz	539.1	$[M – H]^-$	31.15	(92 %)	8.07	(93 %)

[a] Negative ion plasma desorption MS. [b] System A: Nucleosil RP-18 column with eluent A, 0.1 M triethylammonium acetate buffer and eluent B, acetonitrile (gradient: 0–15%, 30 min). [c] System B: Macherey-Nagel ET125/4 Nucleosil 4000-7 PEI column with eluent A, 0.01 M Tris/HCl (pH = 8.4) and eluent B, Tris/HCl (pH = 8.4), 1.0 M NaCl.

Phosphorylation reactions were investigated in some detail. It had been reported that reaction of nucleosides with phosphorus oxychloride was somewhat faster in trimethyl phosphate as compared to triethyl phosphate [15]. We investigated the reaction of ethyl derivative **9b** with phosphorus oxychloride under various conditions. Reaction time was always virtually identical in both solvents. Proton sponge accelerated reaction time from 7 to 2 h, while pre-heating of reagents before the addition of phosphorus oxychloride had no effect.

Phosphorylation of **9a–e** to obtain triphosphates **10a–e** yielded a number of side products (*figure 4*). For butyl derivative **10e**, structure elucidation of the major side products was performed as preparation of **10e** yielded the largest quantity of side products. A fraction isolated at a concentration of 0.13–0.16 M triethyl ammonium bicarbonate (TEAB) buffer showed five spots in thin layer chromatography on cellulose-coated plates, all of which contained phosphorus as shown by spraying with a phosphate-specific reagent. Four of the spots showed UV absorption at 266 nm (*table V*). The mass spectra (anionic mode) confirmed triphosphate **10e** as the major product. Several pH-dependent signals were detected in the ^{31}P NMR spectrum. According to Cozzone and Jardetzky [16], the signals could be assigned to the 2′-monophosphate (**11**), the 3′-monophosphate (**12**), the 5′-monophosphate (**13**), and the 2′,3′-cyclomonophosphate (**14**, *figure 5*). The identification of the side products is shown in *table V*.

A fraction isolated at 0.43 M TEAB buffer concentration contained two more side products and a small amount of **10e**. The major side product showed a mass of 600.7. The ^{31}P NMR spectrum in dimethylsulfoxide showed four signals, a triplet at –23.87 ppm (P_β, $J_{P\alpha P\beta}$ = 21.8 Hz, $J_{P\gamma P\beta}$ = 22.9 Hz), a doublet at –11.93 ppm (P_α, $J_{P\alpha P\beta}$ = 21.8 Hz), a doublet at –11.39 ppm (P_γ, $J_{P\gamma P\beta}$ = 22.9 Hz), and a singlet at 16.41 ppm. These data indicate that the compound (**15**) contains a 2′,3′-cyclophosphate group in addition to the 5′-triphosphate residue of **10e**. The second side product with a molecular mass of 619.1 is a ring-open analogue of **15**, since the ^{31}P NMR spectrum clearly shows a signal in the range of a monophosphate in addition to the 5′-triphosphate structure. Bisphosphorylation at the 2′- and 3′-hydroxyl groups was not observed. The ratio of formed **10e**:**15** was ca. 2:1.

The particularly large amount of side products observed in the preparation of the 5-butyluridine triphosphate **10e** may be due to steric interaction between the bulky butyl residue and the 5′-hydroxyl function in polar aprotic solvents, which leads to an increased phosphorylation of the secondary hydroxyl groups at C2′ and C3′. The preparation of other nucleotides yielded the analogous side products, but in smaller quantities. Use of proton sponge as reaction accelerator was not the cause for the formation of 2′- and 3′-phosphoric acid esters and 2′,3′-cyclophosphates as side products, as we observed the formation of the same compounds in the absence of proton sponge.

In addition to nucleotide side products, large amounts of inorganic phosphates, including cyclometatriphosphate ($P_3O_9^{3-}$), phosphate (PO_4^{3-}), pyrophosphate ($P_2O_7^{4-}$) and linear triphosphate ($P_3O_{10}^{5-}$) were obtained *(table V)*. The stable cyclometatriphosphate was particularly difficult to remove by standard chromatographic methods due to partial coelution with the target UTP derivatives (*figure 4* and *table V*).

Table V. Analysis of isolated fractions obtained from ion exchange chromatography of crude **10e** (compare *figure 3*).

Fraction	I	II	III	IV	V	VI
TEAB concentration [%][a]	0	13–16	31–36	41–44	70–80	80
Yield [mg] (of 1 820 mg crude product)[b]	810	241	250	67	114	33
			Spectroscopic methods			
UV maximum at [nm]	218[c]	266	266	266	266	266
^{31}P-NMR (in D_2O)	–7.3 (s); 2.4 (s); 3.0 (s); 3.1 (s)	(s); 2.8 (s); 2.3 (s); 0.4 (s); 0.0 (s)	–9.8 (d); –11.0 (d); –20.8 (s); –22.4 (t)	21.8 (s); –5.2 (d); –9.8 (d);	4.8 (s); 4.2 (s); 2.2(s);	21.8 (s); 4.5. (s); –8.1 (s)[d]; –10.3 (s)[d];
(pH value)	(pH = 7.2)	(pH = 4.5) 19.2 (s); 4.0 (s); 3.7 (s); 3.5 (s); 2.7 (s) (pH = 9.5)	(pH = 6.2)	–20.8 (t) (pH = 8.0)	–7.7– –10.3 (m); –20.0 (s); –21.7 (s) [d] (pH = 7.4)	–21.7 (s)[d] (pH=8.0)
MS (neg. Mode)	n.d.[e]	379[f]	538[f]	601[f], [619]	[540, 619], 700[f]	760[f]
			Cellulose-TLC (solvent: 2-propanol:NH_3(25 %):H_2O = 6:3:1)			
UV detection at 266 nm	3 spots	4 spots	1 spots	2 spots	4 spots	3 spots
Phosphate detection ($FeCl_3$/5-sulfosalicylic acid reagent)	3 spots	5 spots	2 spots	2 spots	5 spots	5 spots
			Deduced structure			
Inorganic phosphate as determined by ^{31}P-NMR	PO_4^{3-} $P_2O_7^{4-}$	PO_4^{3-}	$P_3O_9^{3-}$		$P_3O_9^{3-}$, PO_4^{3-}, $P_3O_{10}^{5-}$	PO_4^{3-}, $P_3O_{10}^{5-}$
Nucleotides[g] and other organic compounds	phosphates of 1,8-bis-(dimethyl)-ammonium-naphthalene	**11** **12** **13** **14**	**10e**	**15**	structure could not be determined[h]	structure could not be determined[i]

[a] 100% corresponds to 1 M TEAB buffer. [b] Unidentified: 305 mg. [c] Typical spectrum for aromatic compounds. [d] Signal not resolved. [e] n.d. = not determined. [f] Main peak. [g] For structures see *figures 2* and *5*. [h] Structure contains a total of 5 phosphate groups but no 2′3′-cyclic phosphate groups. [i] Structure contains a total of 6 phosphate groups (one of them is a 2′3′-cyclic phosphate group).

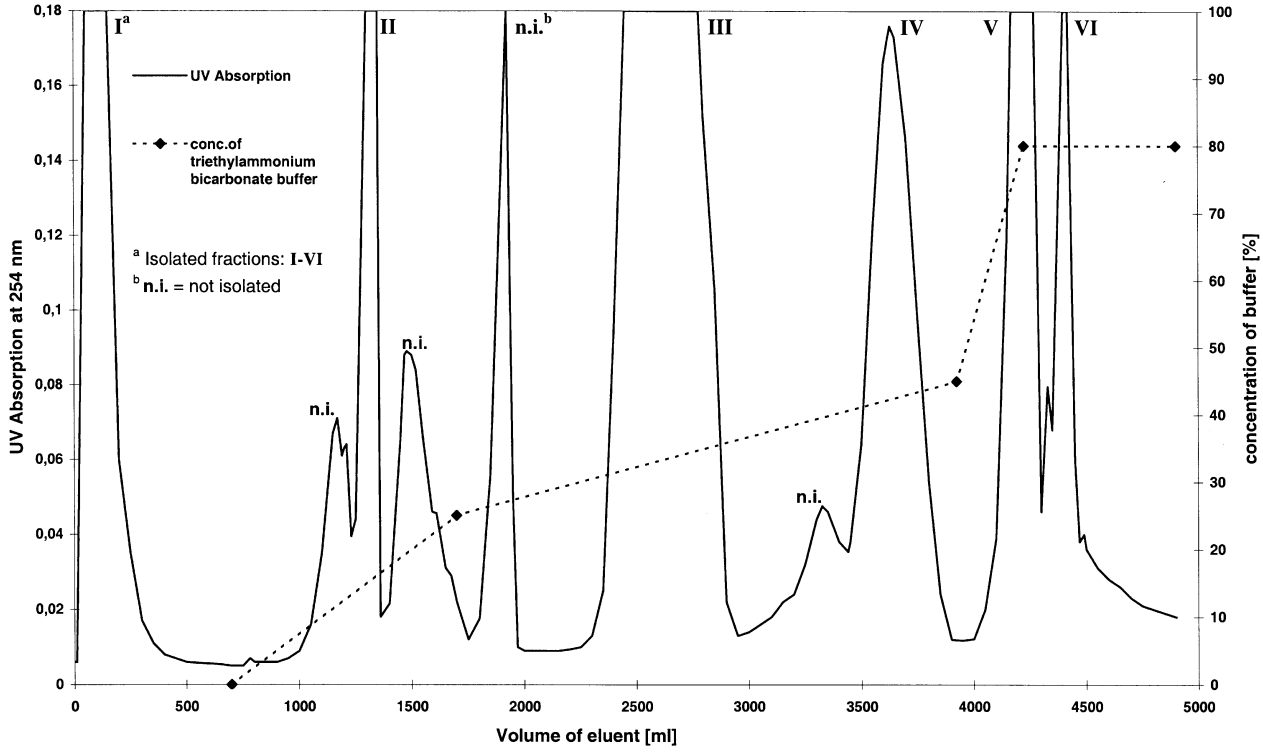

Figure 4. Separation of crude **10e** on DEAE-Sephadex A25 by FPLC.

3. Biological evaluation

$P2Y_2$ receptor activity was determined in a mouse neuroblastoma × glioma hybrid cell line (NG 108-15) by fluorimetric measurement of the increase in intracellular calcium concentration caused by stimulation of $P2Y_2$ receptors via activation of phospholipase C. Selected compounds were additionally tested in a human cystic fibrosis epithelial airway cell line (CF/T43) and a human basal epithelial airway cell line (BEA).

4. Results and discussion

4.1. Neuroblastoma × glioma cells (NG108-15 cell line)

The putative physiological $P2Y_2$ receptor agonists UTP (**1**) and ATP (**4**), the ATP analogue ZTP (**5**), uridine diphosphate UDP (**2**) and the corresponding monophosphate UMP (**3**) were investigated at NG108-15 cells for comparison. Initially, single concentrations (50 and/or 500 μM) of UTP derivatives and standard nucleotides were used *(table VII)*. Before testing it was shown that not even at high concentrations (500 μM) did the inorganic phosphates pentasodium triphosphate ($Na_5P_3O_{10}$), trisodium tricyclometaphosphate ($Na_3P_3O_9$), and sodium pyrophosphate ($Na_4P_2O_7$), which could be present as side products in some of the nucleotides, show any effects. As previously shown, UTP acted as a potent $P2Y_2$ receptor agonist, exhibiting an EC_{50} value of 1.25 μM and a maximal increase in intracellular calcium of 69% *(table VIII)*. The observed potency for UTP is in accordance with published data [5, 17]. ATP was somewhat less potent, exhibiting an EC_{50} value of 17.7 μM, but showed about the same maximal stimulation as UTP. The lower activity of ATP may be due to faster enzymatic degradation of ATP as compared to UTP under test conditions [18, 19]. The ring-open, base-modified ATP analogue ZTP (**5**) was found to be nearly equipotent to ATP in our assay system.

In the system described, addition of UDP (**2**) also resulted in an increase in intracellular calcium concentration, with an EC_{50} value of 3.2 μM *(table VIII)*. Efficacy, however, was only 61% of that of UTP. UDP has previously been shown to be inactive at $P2Y_2R$ [19, 20], but it might have been contaminated with UTP, or could have been phosphorylated enzymatically, and the result-

Table VI. Crystal data of compound **8d.**

Empirical formula	$C_{33}H_{30}N_2O_9$
Formula weight	598.59
Temperature	173 (2) K
Wavelength	MoKα, 71.073 pm
Crystal system	orthorhombic
Space group	$C222_1$
Unit cell dimensions	a = 1 482.37 (7) pm α = 90 deg. b = 2 322.16 (14) pm β = 90 deg. c = 1 780.29 (13) pm γ = 90 deg.
Volume	6.1283 (6) nm^3
Z	8
Reflections used for cell refinement	25
Density (calculated)	1.298 Mg/m^3
Absorption coefficient	0.095 mm^{-1}
F(000)	2 512
Crystal size	0.3 × 0.2 × 0.2 mm
Theta range for data collection	2.29–25.05 deg.
Index ranges	$-17 \le h \le 17$, $-27 \le k \le 27$, $-21 \le l \le 21$
Reflections collected	20 046
Independent reflections	5 425 [R(int) = 0.0561]
No. of standard reflections / decay	3 / 0 %
Completeness to 2Theta = 25.05	99.6 %
Absorption correction	N/a
Refinement method	Full-matrix least-squares on F^2
Treatment of hydrogen atoms	mixed[a]
Data / restraints / parameters	5 425 / 203 / 436
Goodness-of-fit on F^2	0.912
Final R indices [I > 2sigma(I)][b]	R1 = 0.0392, wR2 = 0.0835
R indices (all data)[b]	R1 = 0.0638, wR2 = 0.0913
Absolute structure parameter	–0.5(9)
Extinction coefficient	0.0017(2)
Largest diff. peak and hole	157 and –201 $e.nm^{-3}$
Diffractometer:	ENRAF-NONIUS CAD4
Program:	SHELXS-93 [28], SHELXL-97 [29]

[a] See Experimental. [b] Definition of R values:
$R1 = \Sigma \| F_o| - |F_c \| / \Sigma |$ and $wR2 = \{\Sigma w(F_o^2 - F_c^2)^2 / \Sigma w(F_o^2)^2\}^{1/2}$; $w = 1/\{\sigma^2(F_o^2) + (0.0494 \cdot P)^2\}$; $P = (Max(0, F_o^2) + 2F_c^2)/3$.

ing UTP may have been responsible for the effects measured. Uridine monophosphate (UMP, **3**) exhibited only very weak activity at high concentrations of 500 μM, which might, again, be due to contamination by UTP and/or enzymatic conversion to UTP [18, 19].

5-Alkyl-substituted UTP derivatives showed lower activity at $P2Y_2$ receptors than UTP. Activity decreased with increasing size of the 5-substituent exhibiting the following rank order of potency: UTP > 5-methyl-UTP > 5-ethyl-UTP > 5-isopropyl-UTP > 5-propyl-UTP > 5-butyl-UTP *(table VII)*. A recorded dose-response curve for 5-ethyl-UTP (**10b**) showed this compound to be a full agonist at $P2Y_2R$ of NG108-15 cells exhibiting an EC_{50} value of 99 μM *(table VIII)*.

4.2. CF/T43 and basal epithelial airway (BEA) cells

Selected compounds were further tested in CF/T43 cells [4], a human epithelial airway cell line containing the defective chloride channel (CFTR), that causes cystic fibrosis, and compared with a basal epithelial airway (BEA) cell line. Results from measurements of $P2Y_2R$-mediated increase $[Ca^{2+}]_i$ were virtually identical in CF/T43 and BEA cells *(tables IX* and *X)*. Activity of nucleotides and maximal increase in $[Ca^{2+}]_i$ was higher in CF/T43 and BEA cells as compared to NG108-15 cells. ATP was found to be nearly equipotent to UTP in CFT/43 and BEA cells *(table IX)*, while ZTP was somewhat less potent *(table X)*. 5-Methyl-UTP (**10a**) showed a dose-

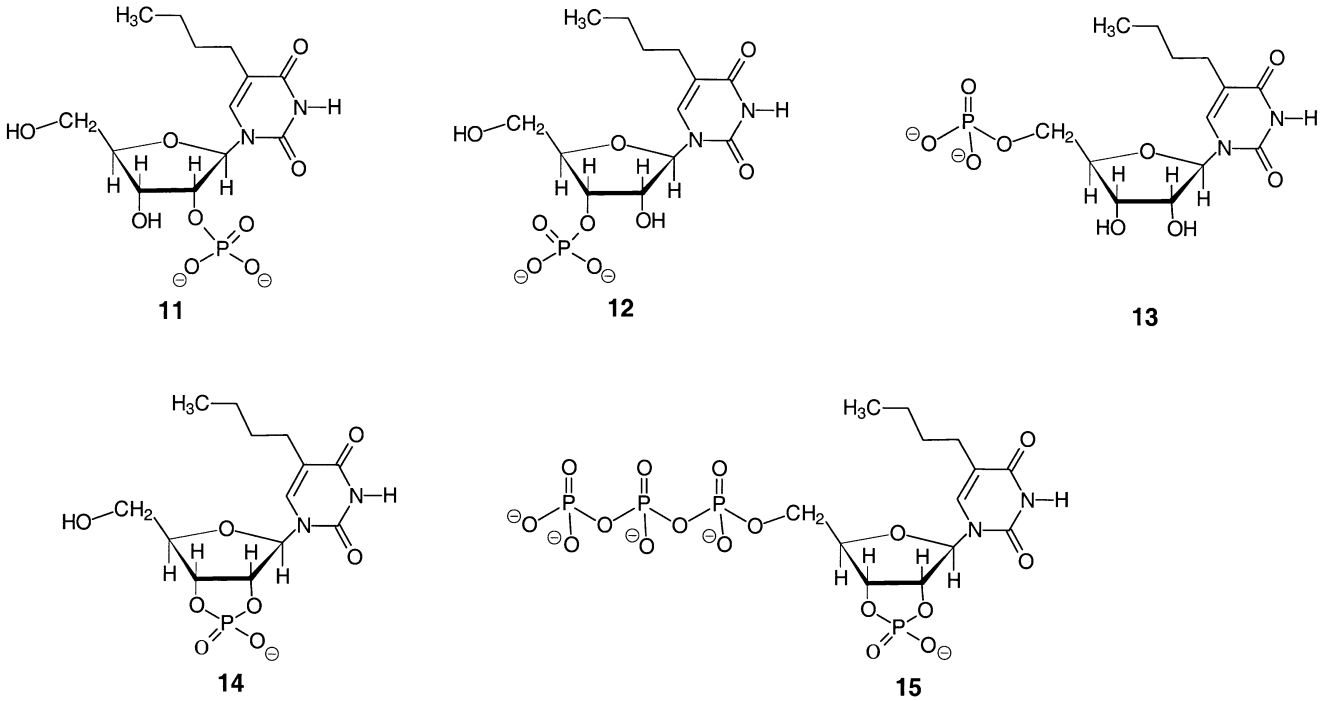

Figure 5. Structures of identified side products in the phosphorylation of **9e** (preparation of **10e**).

dependent increase in $[Ca^{2+}]_i$ and appeared to be nearly equipotent to ATP and UTP *(table X)*, while 5-ethyl-UTP (**10b**, 10–100 nM) only slightly increased $[Ca^{2+}]_i$ in BEA cells *(table X)*.

The higher potency of nucleotides in epithelial airway cells as compared to NG108-15 cells may reflect species differences (human, mouse). Differences in enzyme pattern and enzymatic activity of nucleotidases and phosphatases may also contribute to the differences measured [18, 19, 21]. A further factor, which has to be taken into account, may be differences in techniques used for the measurements. Thus, NG108-15 cells were used in

Table VII. Effects of nucleotides on $P2Y_2$ receptor-mediated increase in intracellular calcium concentration in NG108-15 cells, results from testing of single concentrations of compounds.

Compound[a]		Percent increase in $[Ca^{2+}]_i \pm$ SEM (number (*n*) of independent experiments)	
		50 μM concentration of test compound	500 μM concentration of test compound
1	UTP	69.3 ± 8.2 (*n* = 10)	(179.0 ± 26.9)[b] (*n* = 5)
2	UDP	42.4 ± 4.5 (*n* = 4)	31.3 (*n* = 1)
3	UMP	n.d.[c]	10.6 ± 1.3 (*n* = 2)
4	ATP	44.6 ± 5.9 (*n* = 3)	67.2 ± 17.9 (*n* = 2)
5	ZTP	54.3 ± 13.5 (*n* = 2)	n.d.
10a	5-Methyl-UTP	n.d. 52.0 ± 29.7 (*n* = 2) at 100 μM	n.d.
10b	5-Ethyl-UTP	28.9 ± 7.8 (*n* = 3)	71.7 ± 12.0 (*n* = 3)
10c	5-Propyl-UTP	0 (*n* = 2)	38.6 ± 5.3 (*n* = 3)
10d	5-Isopropyl-UTP	n.d.	46.2 ± 25.0 (*n* = 2)
10e	5-Butyl-UTP	n.d.	25.0 ± 0.7 (n = 3)

[a] For structures see *figures 1* and *2*. [b] High values are due to lysis of cells observed at a concentration of 500 μM of UTP. [c] n.d. = not determined.

Table VIII. Effects of nucleotides on $P2Y_2$ receptor-mediated increase in intracellular calcium concentration in NG108-15 cells, results from dose-response curves.

	Compound	EC_{50} [μM][a] (95 % confidence intervals)	Maximal effect in % of max. UTP effect (= 100 %) (number (*n*) of independent experiments)
1	UTP	1.25 (0.11–14)	100 ± 12 (*n* = 10)
2	UDP	3.21 (0.28–36)	61 ± 7 (*n* = 4)
4	ATP	17.7 (5.6–56)	95 ± 12 (*n* = 3)
5	ZTP	17.1[b]	78 ± 19 (*n* = 2)
10b	5-Ethyl-UTP	99 (20–480)	104 ± 17 (*n* = 3)

[a] Results from three independent experiments unless otherwise noted. [b] Single dose-effect curve.

suspension while CF/T43 and BEA cells were used as attached cell layers in culture dishes (see Experimental protocol). It has been shown that stressing of cells, e.g,. by agitation, may result in a massive release of endogenous nucleotides [22], a fact which clearly affects the test results obtained with exogenously applied nucleotides. Such variations in EC_{50} values for nucleotides, e.g., UTP and ATP, at $P2Y_2R$ in different test systems have been described [5]. In the present study, degradation of compounds was not investigated, though enzymatic and chemical hydrolysis undoubtedly play a role [21]. Calcium measurements were, however, performed very fast, within seconds up to a few minutes, and therefore, only moderate degradation will have occurred. It had been shown that in airway epithelial cells, where strong UTP degradation is observed, after 5 min, about 70% of intact UTP is still present [21].

Table IX. Effects of standard nucleotides on $P2Y_2$ receptor-mediated increase in intracellular calcium concentration in CF/T43 cells and basal epithelial airway (BEA) cells, results from dose-response curves.

Compound	Cell line	EC_{50} [μM] (95 % confidence intervals)[a]
1 UTP	CF/T43cells	0.10 (0.01–0.93)
	BEA cells	0.16 (0.005–5.6)
4 ATP	CF/T43cells	0.17 (0.01–2.9)
	BEA cells	0.20[b]

[a] Determined in 3–4 separate experiments unless otherwise noted. [b] Two separate experiments.

4.3. Structure-activity relationships

The $P2Y_2R$ is unique in that it is stimulated by purine (ATP) as well as pyrimidine nucleotides (UTP). We confirmed previous findings [5, 20, 22, 23] that UTP (**1**) and ATP (**4**) activate $P2Y_2R$ in low micromolar to submicromolar concentrations (EC_{50} of UTP: 1.25 μM at NG108-15 cells, 0.10 μM at CF/T43 cells, and 0.16 μM at BEA cells; EC_{50} of ATP: ca. 18 μM at NG108-15 cells, and ca. 0.2 μM at CF/T43 and BEA cells, see *tables VIII* and *IX*). Efficacy was similar for both physiological agonists. A ring-open analogue of ATP, ZTP (**5**) exhibited similar potency as ATP indicating that purine base modification was possible without loss of activity. Truncation

Table X. Effects of nucleotides on $P2Y_2$ receptor-mediated increase in intracellular calcium concentration in CF/T43 cells and BEA cells, results from testing of single concentrations of compounds

Compound	Cell line	Percent increase in $[Ca^{2+}]_i$ ± SEM (number of independent experiments) 10 nM concentration of test compound	100 nM concentration of test compound
1 UTP	CF/T43cells	108 ± 80 (*n* = 3)	197 ± 58 (*n* = 3)
	BEA cells	110 ± 49 (*n* = 3)	173 ± 113 (*n* = 3)
4 ATP	CF/T43cells	103 ± 20 (*n* = 3)	266 ± 94 (*n* = 3)
	BEA cells	199 ± 94 (*n* = 3)	208 ± 42 (*n* = 3)
5 ZTP	CF/T43cells	36 ± 29 (*n* = 2)	117 ± 55 (*n* = 2)
	BEA cells	80 ± 35 (*n* = 2)	138 ± 22 (*n* = 2)
10a 5-Methyl-UTP	CF/T43cells	155 ± 46 (*n* = 2)	269 ± 24 (*n* = 2)
	BEA cells	113 ± 32 (*n* = 2)	312 ± 15 (*n* = 2)
10b 5-Ethyl-UTP	CF/T43cells	39 ± 11 (*n* = 2)	43 ± 26 (*n* = 2)
	BEA cells	17 ± 24 (*n* = 2)	41 ± 7 (*n* = 2)

of the triphosphate chain in UTP to UDP (**2**) and further to UMP (**3**), led to a decrease or loss in activity as reported [5, 20, 22], suggesting that the four negative charges are important for electrostatic interactions with the receptor protein. Only few synthetic UTP analogues have previously been investigated as $P2Y_2R$ ligands [5, 6, 21, 22]. Exchange of the bridging β-γ-oxygen atom in the triphosphate chain by NH, CH_2, or CF_2, respectively, in order to enhance stability towards nuceotidases, have led to a decrease in activity [23]. The only substitution tolerated in the phosphate chain was the replacement of a γ-oxygen atom by sulfur, as in UTPγS [21]. The compound was nearly as potent as UTP itself. A series of UTP derivatives in which the oxygen in the 4-position of the uracil moiety was replaced by various substituents, including (alkyl)amino, (alkyl)thio or alkoxy, had been investigated, but all of the derivatives were less potent than UTP [6].

A 5-substituted UTP derivative that had been investigated was 5-bromo-UTP. It was found to be less potent than UTP or ATP at $P2Y_2R$ [22]. The present study shows that alkyl substituents in the 5-position of UTP are not tolerated by the receptors either. Introduction of an ethyl group in the 5-position of UTP, for example, decreased activity at $P2Y_2R$ of NG108-15 cells ca. 80-fold (from an EC_{50} for UTP of 1.25 μM to 99 μM for 5-ethyl-UTP **10b**). With increasing volume of the 5-substitutent $P2Y_2$ activity was decreased *(table VII)*. Since both polar 5-substituents, such as bromo, and non-polar, especially bulky alkyl substituents, led to decreased activity, it can be concluded, that steric reasons, i.e., lacking bulk tolerance of the receptor in that area, are responsible for this effect.

5. Conclusion

Methods and conditions for the preparation and purification of 5-substituted UTP derivatives were investigated and optimized. New spectroscopic data on UTP derivatives are presented, including ^{13}C and ^{31}P NMR data. 5-Substituted UTP derivatives were found to be full agonists at $P2Y_2$ receptors of NG108-15 cells, and basal epithelial airway cells without or with defective CFTR channel (CF/T43 cell line). Potency of 5-substituted UTP derivatives decreased with increasing volume of the 5-substitutent.

It is planned to investigate the potency of 5-substituted UTP derivatives at other P2Y receptor subtypes, such as $P2Y_4$ or $P2Y_6$. The presented SAR of UTP derivatives may contribute to the design of selective ligands for subtypes of the uracil nucleotide-sensitive P2Y receptors.

6. Experimental protocols

6.1. Chemistry

Melting points were determined with a Büchi 530 apparatus and are uncorrected. Nuclear magnetic resonance spectra were determined using a Bruker AC-200 spectrometer (^1H: 200 MHz, ^{13}C: 50.3 MHz). Chemical shifts are given in ppm downfield from tetramethylsilane as internal standard. ^{31}P-NMR spectra were recorded on a Bruker AMX 400 spectrometer at 161 MHz with H_3PO_4 as an internal standard. UV spectra were recorded with a Perkin Elmer Lambda 12 spectrometer. HPLC was performed using the following equipment: Pharmacia 2249 gradient pump, 2141 variable wavelength monitor set to 266 nm, and a 2221 integrator. Purity controls were performed on two systems: system A: Nucleosil RP-18 column with eluent (A) 0.1 M triethylammonium acetate buffer, and eluent (B) acetonitrile/H_2O (gradient: 0–15%, 30 min). System B: Macherey-Nagel ET125/4 Nucleosil 4000-7 PEI column with eluent (A) 0.01 M Tris/HCl (pH 8.4) and eluent (B) 0.01 M Tris/HCl (pH 8.4), 1.0 M NaCl. Negative ion plasma desorption mass spectra were obtained on Applied Biosystem BIO-ION 20 plasma desorption mass spectrometer, using ^{252}Cf as source of fission fragments. Nucleotides were purified on a Pharmacia High Load system using a triethyl ammonium hydrogen carbonate buffer gradient (0–80%). Thin layer chromatography was performed on silica gel F_{254} (Merck), and in some cases on cellulose TLC plates (Merck). The following solvent systems were used for development of the TLC:

(S1) dichloromethane:methanol = 9:1 for compounds **8a–e**;

(S2) dichloromethane:methanol = 3:1 for compounds **9a–e**;

(S3) 2-propanol:NH_4OH:water = 6:3:1 for compounds **10a–e**, **11–15**.

Phosphate spraying agent (0.1% $FeCl_3$ x 6 H_2O; 7% 5′-sulfosalicylic acid in 75% ethanol) according to Wade and Morgan [24] was used for identification of organic and inorganic phosphates. R_F-values of phosphates were compared to data published by Ebel [25].

6.1.1. General procedure for silylation

A suspension of 5 mmol of uracil derivatives **6a–e** in 20 mL of 1,1,1,3,3,3-hexamethyldisilazane (HMDS) and 1 mL of trimethylsilyl chloride, or a few crystals of $(NH_4)_2SO_4$ respectively, was refluxed until a clear solution was obtained. The solution was allowed to cool, and excess HMDS was removed under reduced pressure. The silylated uracil derivatives **7a–e** were kept under nitrogen. A small sample of the oily sirup was dissolved in

$CDCl_3$ and checked for complete silylation by ^{1}H NMR spectroscopy. Yields ranged from 96–98%.

Selected ^{1}H-NMR data in $CDCl_3$, δ (ppm):

7d: 0.30 (s, 9H, C-O-Si$(CH_3)_3$); 0.32 (s, 9H, C-O-Si$(CH_3)_3$); 1.14 (d, 6H, C5-CH-$(CH_3)_2$, J = 6.9Hz); 2.85 (sept., 1H, C5-CH-$(CH_3)_2$, J = 6.9Hz); 7.99 (s, 1H, C6-H).

6.1.2. General procedure for the synthesis of nucleosides

Silylated uracil derivatives **7a–e** (5 mmol) under nitrogen were dissolved in 5 mL of 1,2-dichloroethane, and 1.30 g (5.5 mmol) of $SnCl_4$ (10% excess) was added with vigorous stirring. 1-O-Acetyl-2,3,5-tri-O-benzoyl-β-D-ribofuranose (2.2 g, 0.4 mmol) in 40 mL of 1,2-dichloroethane was added dropwise to the slightly yellowish solution. The mixture was stirred as indicated below, completion of reaction was controlled by TLC (dichloromethane:methanol = 9:1). Reaction times were between 4–5 h. The reaction solution was poured into a saturated aqueous $NaHCO_3$ solution (ca. 50 mL), or on humidified solid $NaHCO_3$ with successive adding of saturated $NaHCO_3$ solution, respectively, under vigorous stirring, and then allowed to stand overnight. The suspension was filtered over silica gel and the gel was washed twice with 50 mL of dichloromethane and twice with 100 mL of ethyl acetate. The organic phase was separated, dried (Na_2SO_4), filtered over silica gel and evaporated to dryness. The glassy residue was crystallized from methanol, or ethanol respectively, to yield **8a–e**. If necessary, the removal of unreacted sugar and side products was achieved by column chromatography on silica gel using dichloromethane:methanol = 9:1 as eluent. Yields ranged from 81–87%.

Selected ^{1}H-NMR data in DMSO-d_6, δ (ppm):

8b: 0.93 (t, 3H, C5-CH_2-CH_3, J = 7.3 Hz); 2.08 (q, 2H, CH_3, J = 7.3 Hz); 4.64–4.77 (m, 3H, C4′H, C5′H_2); 5.96 (m, 2 H, C2′H, C3′H); 6.21 (d, 1H, C1′H, $J_{1'2'}$ = 3.8 Hz); 7.39–8.04 (m, 16H, C6-H, $H_{aromat.}$); 11.48 (br s, 1H, N1-H, exchangeable).

8c: 0.76 (t, 3H, propyl CH_3, J = 7.1 Hz); 1.33 (sext., 2H, propyl CH_3CH_2-, J = 7.3Hz); 2.05 (t, 2H, propyl $CH_3CH_2CH_2$-, J = 7.2 Hz); 4.61–4.78 (m, 3H, C4′H, C5′H_2); 5.90 (m, 2H, C2′-H, C3′-H); 6.23 (d, 1H, C1′-H, J = 3.7 Hz); 7.38–8.06 (m, 16H, C6H, H_{aromat}); 11.48 (br s, 1H, N3-H, exchangeable).

8d: 1.00 (d, 6H, $CH(CH_3)_2$, J = 6.9Hz); 2.85 (sept., 1H, $CH(CH_3)_2$, J = 6.6Hz); 4.65–4.75 (m, 3H, C4′H, C5′H_2); 6.00 (d, 2H, C3′H, C2′H); 6.25 (d, 1H, C1′H, J = 5.1Hz); 7.01 (d, 1H, C6H, J = 0.9Hz); 7.38–8.05 (m, 16H, C6H, H_{aromat}); 11.47 (br s, 1H, N3-H).

6.1.3. Deprotection of nucleosides

Tribenzoyl nucleoside (**8a–e**, 0.92 mmol) was dissolved in a mixture of 20 mL of absolute methanol and 2.76 mL of 5% methanolic sodium methylate solution. The solution was stirred for 5–8 h and completion of the reaction was determined by TLC (dichloromethane: methanol = 3:1). Neutralisation of the solution was achieved by adding DOWEX-50 WX-8 ion exchange resin washed previously with methanol. After filtering the resin off, 20 mL of water was added and methanol was evaporated. The benzoic acid methyl ester was extracted with diethyl ether and the water fraction was lyophilized to yield the nucleosides **9a–e** in 94–98% yield.

Selected ^{1}H-NMR data in DMSO-d_6, δ (ppm):

5-n-Propyluridine (**9c**): 0.84 (t, 3H, C5-CH_2-CH_2-CH_3, J = 7.3Hz); 1.42 (sext., 2H, C5-CH_2-CH_2-CH_3, J = 7.5 Hz); 2.14 (dt, C5-CH_2-CH_2-CH_3, $J_{1'2'}$ = 7.5 Hz); 3.49–3.68 (m, 2H, C5′H_2); 3.82 (q, 1H, C4′H, J = 3.46/2.94Hz); 3.96–4.03 (m, 2H, C2′H, C3′H); 5.06, 5.33 (br s, 3H, OH (exchangeable)); 5.77 (d, 1H, C1′H, J = 5.3 Hz); 7.73 (s, 1H, C6H); 11.24 (br s, 1H, N3-H (exchangeable)).

6.1.4. Phosphorylation

Synthesis of nucleoside 5′-triphosphate synthesis was adapted from literature procedures [10, 26, 27].

6.1.5. Preparation of tri-n-butylammonium diphosphate

Sodium diphosphate decahydrate (6.69 g; 15 mmol) was dissolved in 150 mL of water (twice distilled). Excess of Dowex ion exchange resin 50 × 8, 20–50 mesh, proton form, prewashed several times with water, was added to the solution of sodium diphosphate, and the mixture was gently stirred for 60 min. A mixture of 60 mL of ethanol and 7.14 mL of tributylamine in a flask was placed in an ice-water bath, and the diphosphate solution was filtered directly into the flask. The resin was repeatedly washed with water until the filtrate was no longer acidic. The solvent was then evaporated under vacuum at 40 °C, yielding a thick, nearly colourless syrup. This residue was treated twice with 100 mL of ethanol and then evaporated. The residue was taken up in 40 mL of dimethylformamide (DMF, anhydrous grade, from Fluka) and evaporated again. This residue was taken up in 30 mL of anhydrous DMF, yielding 30 mL of 0.5 M tri-n-butylammonium diphosphate in DMF. The solution was stored sealed and cooled at 4 °C until used.

6.1.6. Preparation of triethylammoniumhydrogencarbonate (TEAB) buffer

A 1 M solution of TEAB was prepared by bubbling CO_2 through a 1 M triethylamine solution in water at 0–4 °C for several hours (pH approx. 7.4–7.6).

6.1.7. Preparation of nucleotides **10a–e**

Lyophilized nucleoside (**9a–e**, 1 mmol) was dissolved in 5 mL of trimethyl phosphate (dried over 10 Å molecular sieve). The mixture was stirred at room temperature under nitrogen and then cooled to 4 °C. Dry 1,8-bis(dimethylamino)naphtalene ('proton sponge', 0.32 g, 1.5 mmol) was added, followed by 1.3 mmol (0.20 g) of $POCl_3$, 5 min later. After several hours of stirring at 0–4 °C, tri-n-butylamine (0.1 mL, 0.72 mmol) was added to the solution followed by 10 mL (5 mmol) of 0.5 M tri-n-butylammonium diphosphate solution in DMF. After 2–5 min the mixture was poured into 0.5 M cold aqueous TEAB solution (30 mL, pH 7.5) and stirred at 0–4 °C for several minutes.

The solutions were allowed to reach room temperature with stirring and were then left standing for 1 h. Trimethylphosphate was extracted with t-butylmethyl ether and the aqueous solutions were evaporated and lyophilized to yield glassy colourless oils. The reactions were controlled by TLC using freshly prepared solvent system S3. TLC plates were dried before UV absorption was detected and the plates were subsequently sprayed with phosphate reagent.

6.1.8. Purification of nucleotides

The crude nucleoside 5′-triphosphates were purified by ion exchange column chromatography using DEAE-Sephadex A25 (Pharmacia) HCO_3^--form swelled in 1 M NH_4HCO_3 solution at 4 °C. After equilibrating the column with deionized water, the crude product was dissolved in 5 mM aqueous triethylammonium carbonate buffer. The column was washed with deionized water, followed by a solvent gradient of 0–800 mM TEAB in approximatly 3 000 mL of solvent to elute the triphosphates. Fractions were collected and appropriate fractions pooled, evaporated, diluted in water and lyophilized to yield a product with a 'clear glass' appearance. Purity was assessed by HPLC/UV and ^{31}P NMR spectroscopy. Isolated yields: 33% (**10a**), 24% (**10b**), 37% (**10c**), 40% (**10dd**), 26% (**10e**).

6.1.9. Preparation of sodium salts

Nucleotides (50 mmol) were dissolved in absolute methanol (dried over Mg) and evaporated. This procedure was repeated twice. The solid was then dissolved in 5 mL of absolute methanol with stirring. A 1.5-fold excess of a 1 M sodium iodide solution in acetone was added dropwise. The solution was then diluted with absolute acetone. The formed precipitate was filtered off and washed several times with absolute acetone. The white solid was dried under high vacuum.

6.2. Determination of X-ray structure

Single pure crystals of **8d** were obtained by slow crystallization from ethanol at room temperature over several weeks. Low temperature X-ray intensity data were collected on an Enraf-Nonius CAD4 diffractometer using MoKα radiation. The structure was resolved with direct methods using SHELXS-97 [28] and refined by full-matrix least squares iteration against F^2, using SHELXL-97 [29]. All non-hydrogen atoms were refined anisotropically. The coordinates of hydrogen atoms bonded to C5, C6, C7, and C8 were freely refined using isotropic displacement parameters. For all other hydrogen atoms a riding model was employed in the refinement with their U_{iso} constrained to equal 1.2 times the U_{eq} of the parent atoms (1.5 times U_{eq} in the case of the hydrogen atoms of the methyl groups). Crystallographic data were deposited at the Cambridge Crystallographic Data Centre as supplementary publication (deposition number 120084). Free copies of data are available from: CCDC; 12 Union Road, Cambridge CB21EZ (fax: + 44 1223 336 033; e-mail: deposit@ccdc.cam.ac.uk).

6.3. Biological studies

ATP, UTP, UDP, UMP, and ZTP were purchased from Sigma Chemical Co. in the highest available purity grade. Nucleotides were checked for autofluorescence prior to testing.

6.3.1. NG108-15 cell culture

NG108-15 cells were kindly provided by Berit Färjh, Dept. of Medical Neurochemistry, Lund University Hospital, Sweden. NG108-15 cell line (hybrid cell line generated by fusion of mouse neuroblastoma and C6 glioma cells) was cultured in tissue culture flasks (75 or 150 cm^2). Cells were grown adherent in tissue culture flasks in a 5% CO_2 atmosphere at 37 °C until confluent. The growth medium consisted of a mixture of 500 mL of Dulbecco's modified Eagle medium (DMEM) supplemented with 4.5 g/L of glucose and pyruvate, 55 mL of foetal calf serum, 10 mL of HAT (hypoxanthine, aminopterin, thymidine) supplement (Gibco article No. 15140-114) and 5.5 mL of penicillin/streptomycin (Gibco article no. 21060-017). Medium was changed nearly every day depending on cell density as determined by visual inspection.

6.3.2. Preparation of fura2-loaded cells for measurements

NG108–15 cells were examined under a microscope and cells were used when confluent. The medium was removed from the flask, growth medium (10 mL at 37 °C) was added and the cells were dispersed into a single cell

suspension by gentle, brief, repeated pipetting. The cells were centrifuged and the pellet was resuspended in Krebs-Ringer-Hepes (KRH) buffer (conc. in mM: NaCl 125; KCl 5.0; $MgSO_4$ 1.2; KH_2PO_4 1.2; $CaCl_2$ 2.0; glucose 6.0 Hepes 25; pH adjusted to 7.4, with NaOH) in a concentration of 10^6 cells per mL. The cells were incubated with 2 μM of fura-2/AM for 45 min at 37 °C in the dark, spun down (at 1 000 *g*) and washed twice with the same amount of KRH buffer as used before.

6.3.3. Measurement of $[Ca^{2+}]_i$ using NG108-15 cells in suspension

$[Ca^{2+}]_i$ was determined as described by Lin et al. [30] measuring fluorescence of fura-2 loaded cells (2 mL of cell suspension containing 10^6 cells per experiment, 37 °C) using a Hitachi Model F-2000 dual wavelength fluorescence spectrophotometer. Test compound (10 μL) was added. The additon of $P2Y_2R$ agonists resulted in a transient increase in intracellular calcium concentration. After baseline was reached again, 10 μL of Triton X 100 (10% aqueous solution) was added, followed by the addition of 10 μL of a saturated solution of EGTA and 10 μL of a saturated solution of Tris base. $[Ca^{2+}]_i$ was calculated as described [31].

6.3.4. CF/T43 and BEA cell cultures

Airway epithelial cell lines CF/T43 and BEA (kindly provided by Dr J.R. Yankaskas), which express an endogenous $P2Y_2R$ [4] were routinely grown in 75 cm^2 tissue culture flasks (Costar) using keratinocyte growth medium (KGM; Clonetics, catalog No. CC-3115) at 37 °C in a humidified 4% CO_2 atmosphere. Medium was changed 2–3 times a week depending on cell density, and cells were passaged every 7–10 d. For passaging, cells were washed twice with phosphate-buffered saline (PBS) and then treated with 0.1% trypsin/EDTA for 5–10 min to detach the cells. Soybean trypsin inhibitor (three-fold excess) was used to neutralize trypsin prior to passaging.

6.3.5. Measurement of intracellular calcium in CF/T43 and BEA cell monolayers

Cell culture dishes (20 cm^2) with a confluent monolayer of CF/T43 or BEA cells were washed twice with 2 mL of Krebs-Ringer-Hepes (see above). After the addition of fura-2/AM (2 μM), cells were incubated at 37 °C in the dark for 1 h. The medium was changed to 4 mL of fresh KRH buffer and cells were washed 3 times before being incubated for another 15 min to remove non-hydrolysed dye. Immediately before measurement, the experimental incubation medium was replaced again (2 mL) and the culture dishes were placed in the spectrofluorometer (photon counter; Curt Lindmark Innovation AB, Sweden). After base line stabilization, the test compound was rapidly added with careful shaking, culture dishes were re-inserted within 10 s, and changes in fluorescence were registered until base line levels were reached again (3–10 min). Then, Ca^{2+} -ionophore ionomycin (10 μM) and subsequently $MnCl_2$ (20 mM) were added in order to determine maximum and minimum values of fura-2 fluorescence. Calculations of $[Ca^{2+}]_i$ were made according to Grynkiewicz et al. [31].

Acknowledgements

We thank Gaby Huhurez for skillful technical assistance. C.E. Müller is grateful for support given by the Fonds der Chemischen Industrie and the Industrie- und Handelskammer Würzburg-Schweinfurt. This project was supported by grants from the Deutscher Akademischer Austauschdienst (DAAD) to B.K. and C.E.M. and from the Svenska Institutet to E.H.

References

[1] Fredholm B., Abbracchio M.P., Burnstock G. et al., Pharm. Rev. 46 (1994) 143–156.

[2] Bhagwat S.S., Williams M., Eur. J. Med. Chem. 32 (1997) 183–193.

[3] Abbracchio M.P., Burnstock G., Pharmac. Ther. 64 (1994) 445–475.

[4] Parr C.E., Sullivan D.M., Paradiso A.M., Lazarowski E.R., Burch L., Olsen J.C., Erb L., Weisman G.A., Boucher R.C., Turner J.T., Proc. Natl. Acad Sci. USA 91 (1994) 3275–3279.

[5] Heilbronn E., Knoblauch B.H.A., Müller C.E., Neurochem. Res. 22 (1997) 1041–1050.

[6] Shaver S.R., Pendergast W., Siddiqi S.H., Yerxa B.R., Croom D.K., Dougherty R.W., James M.D., Jones A.N., Rideout J.L., Nucleosides Nucleotides 16 (1997) 1099–1102.

[7] Müller C.E., Stein B., Curr. Pharm. Design. 2 (1996) 501–530.

[8] Järlebark L., Erlandsson M., Uri A., King B.F., Ziganshin A.U., Johansson C., Heilbronn E., Biochem. Biophys. Res. Comm. 229 (1996) 363–369 .

[9] Szemõ A., Szabocs A., Sági J., Ötvös L.J., Carbohydr. Nucleosides Nucleotides 7 (1980) 365–379.

[10] Zimmet J., Järlebark L., Hammarberg T. et al., Nucleosides. Nucleotides 12 (1993) 1–20.

[11] Ludwig L., Acta. Biochim. Biophys. Acad. Sci. Hung. 16 (1981) 131–133.

[12] Mishra N.C., Broom A.D., J. Chem. Soc. Chem. Commun. (1991) 1276–1277.

[13] Bennua-Skalmowski B., Krolikiewicz K., Vorbrüggen H., Tetrahedron. Lett. 36 (1995) 7845–7848.

[14] Hunt D.J., Subramanian E., Acta. Crystallogr. B25 (1969) 2144–2152.

[15] Ikemoto T., Haze A., Hatano H., Kitamoto Y., Ishida M., Nara K., Chem. Pharm. Bull. 43 (1995) 210–215.

[16] Cozzone P.J., Jardetzky O., Biochemistry 15 (1976) 4853–4859.

[17] Conigrave A.D., Jiang L., Cell. Calcium 17 (1995) 111–119.

[18] Harden T.K., Lazarowski E.R., Boucher R.C., Trends. Pharmacol. Sci. 18 (1997) 43–46.

[19] Nicholas R.A., Watt W.C., Lazarowski E.R., Qing L., Harden T.K., Mol. Pharmacol. 50 (1996) 224–229.

[20] Erb L., Lustig K.D., Sullivan D.M., Turner J.T., Weisman G.A., Proc. Natl. Acad. Sci. USA 90 (1993) 10449–10453.

[21] Lazarowski E.R., Watt W.C., Stutts M.J., Stutts M.J., Brown H.A., Boucher R.C., Harden T.K., Br. J. Pharmacol. 117 (1996) 203–209.

[22] Lazarowski E.R., Watt W.C., Stutts M.J., Boucher R.C., Harden T.K., Br. J. Pharmacol. 116 (1995) 1619–1627.

[23] Pendergast W., Siddiqi S.H., Rideout J.L., James M.K., Dougherty R.W., Drug. Dev. Res. 37 (1996) 133 (abstract).

[24] Wade H.E., Morgan D.M., Biochem. J. 60 (1955) 264–270.

[25] Ebel J.P., Bull. Soc. Franc. (1953) 1089–1095.

[26] Moffat J.G., Can. J. Chem. 42 (1964) 599–604.

[27] Kovacs T., Ötvös L., Tetrahedron. Lett. 29 (1988) 4525–4528.

[28] Sheldrick G.M., Acta. Crystallogr. A46 (1990) 467.

[29] Sheldrick G.M., Program for crystal structure refinement, University of Göttingen, 1997.

[30] Lin T.A., Lustig K., Sportiello M.G., Weisman G., Sun G.Y., J. Neurochemistry 60 (1993) 1115–1125.

[31] Grynkiewicz G., Poenie M., Tsien R.Y., J. Biol. Chem. 260 (1985) 3440–3450.